Red-Emitting Phosphors for White LEDs: Optimizing Eu^{3+} Doping via Microwave-Assisted Synthesis

S B Pandey[1], A J Nadgawda[1], C S Khade[2]

[1]*Research Scholar, Department of Physics, G H Raisoni University, India*
[2]*Assistant Professor, Department of Physics, G H Raisoni University, India*
Email: shashib.pandey@raisoni.net

Abstract: Europium-doped calcium molybdate phosphors $CaMoO_4:xEu^{3+}$ were made using the microwave-assisted solid state metathesis mode to enhance their suitability for near-UV-based white LEDs. X-ray diffraction analysis confirmed the formation of well-crystalline phosphors with a scheelite-type structure, indicating uniform incorporation of Eu^{3+} ions into the crystal lattice. The phosphors exhibited strong photoluminescence with a prominent emission peak at 618 nm under 392 nm excitation, attributed to the $^5D_0 \rightarrow {}^7F_2$ transitions of Eu^{3+} ions. Optimization experiments determined that an 0.08mol% doping concentration of Eu^{3+} ions maximized the luminescence intensity, showcasing efficient energy transfer mechanisms within the material. The phosphors demonstrated favorable color rendering capabilities, as evidenced by their chromaticity coordinates (x = 0.668, y = 0.323), which closely approached NTSC standards. Fluorescence lifetime analysis revealed a mono-exponential decay curve with a lifetime of 0.401 ms for the $^5D_0$ excited state of Eu^{3+}. Overall, microwave-assisted synthesis enabled the production of homogeneous phosphors with fine structural characteristics, offering significant advantages in terms of efficiency and performance for future applications in solid-state lighting devices. These phosphors hold promise for enhancing the red component in LED technology, contributing to advancements in energy-efficient and high-quality lighting solutions.

Keywords: Luminescent, Phosphors, Solid State Metathesis Synthesis, wLED.

1. Introduction

Over the past decade, LED lights have become incredibly popular worldwide because they are good for the environment and help save energy. Due to their remarkable luminous efficiency, enhanced lifetime, lower consumption of electricity, and environmental friendliness when compared to conventional incandescent or fluorescent bulbs, diodes emitting white light,, have received significant attention in the lighting field and display industry[1-3].

At present, the blue LED chip having (InGaN) base with ($YAG:Ce^{3+}$) a yellow phosphor is used to create the most popular commercial w-LEDs[4-6]. The development of these revolutionary lighting and display technologies has been significantly aided by phosphor materials.

However, this method of converting white light contains some negatives like lower color rendering index, thermal stability issues, spectral gaps, color temperature variations, efficiency loss, blue light hazards, and phosphor material degradation over time. These negatives is due to due to insufficient red-light sources. To overcome these challenges and improve the versatility of white light-emitting diodes (WLEDs), some other method is used. These methods involve the chips having near-ultraviolet (NUV) and ultraviolet (UV) to activate tricolored (RGB) and the red-green mixed materials (phosphors), which are then stimulated by blue chips. Therefore, the research is going on to develop red light-emitting luminescent materials with very good absorption capabilities for near UV/UV and blue light. These materials have great applications in the display, lighting, surface painting, and coating industries.

For LED lighting, researchers have studied rare earth doped oxide oxides and compounds containing molybdate. Because of its exceptional morphologically, chemically and thermally stability, exceptional luminescence efficiency, and exceptional color purity, rare earth doped oxide materials are also utilized in a wide range of display device applications [7, 8].These substances frequently act as homes for fluorescent ions with the intention of producing particular emission characteristics, most notably bright red phosphors. These investigations concentrate on the red component, which can produce white light when paired with blue and green phosphors and a UV diode.

The optical properties of these oxide lattices are because of the 4f electrons of rare earth ions. Therefore, these materials find extensive use in various fields of biological probes, optical transmission, and medical diagnosis [9].

Solid state reactions [10–12], sol–gel [13,14], soft-chemical [15], precipitation [16], solvothermal [17–18], spray pyrolysis [18–20], and combustion [19–20] are the common methods used to synthesize phosphor materials. In order to obtain finer particles, all of these approaches require a lengthy heating process at high temperatures that results in huge aggregates that need to be ground. The process of microwave-assisted synthesis is based on volumetric heating that is selective and caused by electromagnetic radiation interacting with the material. Rapid heating rates and short temperature gradients made possible by microwave heating result in materials that are homogeneous and well-formed quickly. The microwave-assisted synthesis of luminescent inorganic materials can greatly benefit from its high uniformity, varied morphology, and quick screening of various compositions[21]. The microwave aided solid state metathesis reaction process has garnered significant attention among the aforementioned procedures because it requires less reaction time, operates reaction at a relatively low temperature (600°C), and produces large homogenous fine-sized products.

Here, in the present work, we used microwave assisted solid state metathesis synthesis method for the synthesis of $CaMoO_4:Eu^{3+}$ nanomaterial. The produced materials are further characterized by photoluminescence (PL) spectra, FTIR, scanning electron microscopy (SEM) photographs Report Word and X-ray diffraction profiles (XRD). The produced phosphor particles have a high luminous efficiency and are found in the nano range.

2. Materials and Experimental Process

The samples $CaMoO_4:xEu^{3+}$ (with x values of 0.02, 0.04, 0.06, 0.08 and 0.10) were synthesized through a solid-state metathesis reaction utilizing a microwave oven. Solid-state metathesis reactions are often conducted at elevated temperatures, and using a microwave oven can help to achieve these temperatures quickly and efficiently.. For the preparation of the present samples all reagent that includes the Calcium Chloride - $CaCl_2$ (99.9%), Sodium Molybdate Na_2MoO_4 (99.9%), and Eu_2O_3 (99.99 %), were of analytical quality. They are mixed in a pestle and mortar with the right stoichiometric proportions. The paste is then put into the silica crucible after being well mixed using the mortar and pestle. Finally, we kept the powdered sample in the microwave for 15 minutes. When the reaction gets completed, the powder

underwent multiple washes with double distilled water and with the liquid ethanol. Then dried keeping the sample overnight at 90 °C inside the oven. Subsequently, it was removed and left to cool to room temperature. After the sample has cooled, it is grounded one more time in the agate mortar. Here is the reaction for the synthesis of calcium dimolybdate using solid-state metathesis:

$$CaCl_2 + Na_2MoO_4 \xrightarrow{\text{Microwave}} CaMoO_4 + 2NaCl \text{ (by product)}$$

The thus obtained samples were put to use in the scientific analysis. The obtained samples were collected for further analysis and discussion.

3. Structural analysis and Result

$CaMoO_4:xEu^{3+}$ (x = 0.02, 0.04, 0.06, 0.08, and 0.10 mol%) XRD profiles are shown in Figure 1. The locations of the X ray diffraction lines of the prepared product be situated almost identical. Samples doped with $CaMoO_4$ have XRD patterns that match the tetragonal scheelite diffraction pattern (JCPDS card no. 29-0351). As can be seen from the XRD pattern, Eu^{3+} ions have little effect on the host's structure. This shows that doped Eu^{3+} ions penetrated homogeneously into the crystal lattice of $CaMoO_4:0.08Eu^{3+}$ ions take the place of Ca^{2+} ions due to their identical ionic radii (0.107 nm vs. 0.112 nm). According to the high crystalline property of the prepared $CaMoO_4:xEu^{3+}$ sample, restricted Eu^{3+} doping does not alter the crystal structure of synthesised phosphors in any meaningful way.

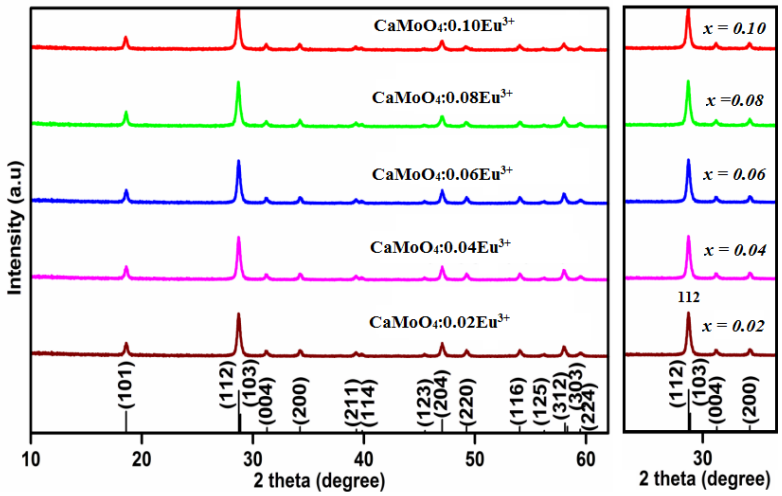

Figure 1. *XRD of $CaMoO_4:xEu^{3+}$*

The average sizes of the crystallite of the Europium doped CaMoO4 vary from approx. 19.18 nm to 40.01 nm which was obtained by using the Scherrer's equation

$$D = 0.9\,\lambda / \beta \cos\theta$$

As the average sizes of the crystallite of the Europium doped $CaMoO_4$, that is calculated by vary from approx. 19.18 nm to 40.01 nm, this result implies that the as synthesized particles can be used in future lighting devices. The preferential orientation (1 1 2) reflection peak was found shifted towards the lower-angle side from 29.2° to 28.7°, which suggests that the successful incorporation of Eu^{3+} ions into the lattice site. The lattice parameters of the as-prepared samples for varying dopant concentrations of Eu^{3+} ions were estimated and shown in Table 1.

Table 1. *Lattice parameter of $CaMoO_4:xEu^{3+}$ phosphors prepared by microwave assisted solid state metathesis synthesis*

Concentration of Eu^{3+} ion	2ϴ (°)	d (Å)	Lattice constant (Å)	Volume (Å^3)
0.02	29.2	3.055	7.485	419.6
0.04	29.0	3.080	7.536	427.5
0.06	28.8	3.097	7.578	435.1
0.08	28.7	3.109	7.605	440.5
0.10	28.9	3.090	7.567	433.4

It is observed that when the doping concentration of Eu^{3+} ion increases, the value of lattice constant and volume of unit cell increases up to the x = 0.08, but if the doping concentration is increased further, the lattice parameter and unit cell volume found to be decreasing. The reason behind is that, the dominant dopant may be occupied largely in the interstitial positions as compared to the substitution position in the host lattice which leads to the compressive strains [22].

4. Luminescence analysis

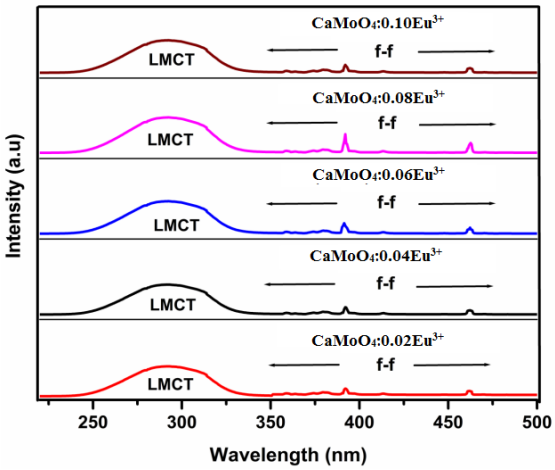

Figure 2. *PL Excitation spectra of $CaMoO_4:xEu^{3+}$ phosphors for different concentration of Eu^{3+}, monitored at emission wavelength 618 nm.*

$CaMoO_4:xEu^{3+}$ phosphors excitation spectra when monitored at wavelength 618 nm wavelength, as depicted in Figure 2, reveal strong absorptions at the wavelength 392 nm and 462 nm. The spectrum presents two distinct regions: a dominant and broader excitation band spanning from 220 nm to 355 nm, and sharp peaks with lower intensity covering the range from 345 nm to 495 nm. The $^7F_0 \rightarrow {}^5L_6$ and $^7F_0 \rightarrow {}^5D_2$ transitions of Eu^{3+} are responsible for these absorptions. which are in good alignment with the near Ultra Violet or blue output wavelengths of GaN-based LED devices.

Two Charge Transfer (CT) bands overlap in the first range, which is between 220 and 355 nm. One CT band moves from the 2p orbital of an oxygen to the unoccupied 4f orbit of europium, and the next CT is a ligand-to-metal transition from oxygen to molybdenum ion. The latter transition indicates the involvement of the Eu^{3+} ions in the excitation process. The second region (345 nm to 510 nm) shows weaker, sharper lines corresponding to typical intra-4f conversions of Eu^{3+} within the host matrix. These transitions are characterized by their distinct spectral features. This alignment holds significant promise for potential applications in LED technology. These results not only deepen our insight into the luminescent properties of these phosphors but also reveal their potential for practical implementation in optoelectronic devices.

The focus of this study is specifically on the near-Ultraviolet or blue GaN based LED phosphors, with specific attention given to their spectroscopic properties within the 345-510 nm range. Presented in Figure 3 are the photoluminescence (PL) spectra of $CaMoO_4:xEu^{3+}$ (x

is concentration of RE^{3+}) when excited with wavelength of 392 nm (near-UV). While the photoluminescence spectra exhibit similarities in shape and peak positions across synthesized samples, except the differences arise in their highest intensities.

Observations within the emission spectra (PL) reveal very sharp lines covering 550 nm to 650 nm, indicative of the transfer from $^5D_0 \rightarrow {}^7F_J$ (where J is taking the values as 1, 2, 3, 4), that take place when the Eu^{3+} ion jump from the higher energy state of to the lowest state or ground state. Notably, primary peak in emission spectra at 618 nm corresponds the transitions $^5D_0 \rightarrow {}^7F_2$ of Eu^{3+}, while $^5D_0 \rightarrow {}^7F_1$ and $^5D_0 \rightarrow {}^7F_3$ occurs within the 550 nm to 650 nm range are comparatively weaker.

The sensitivity of the $^5D_0 \rightarrow {}^7F_2$ electric dipole transition of Eu^{3+} ions is notably dependent on the local environment. This transition is particularly influenced by the absence of symmetry, which allows the orbitals of 4f to blend with orbitals of contrasting parity. This mixing is what enables the electric dipole transition to occur.

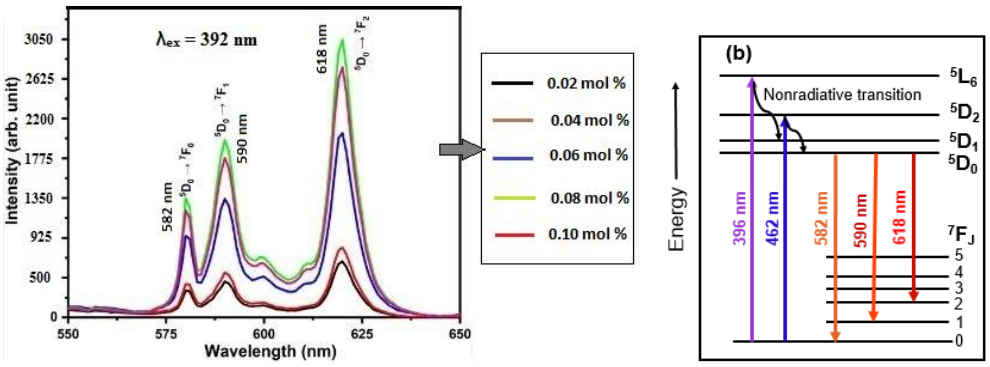

Figure 3. *(a) Emission spectra (PL) of $CaMoO_4:xEu^{3+}$ phosphors monitored at the excitation wavelength 392 nm. (b) Energy level diagram of Eu^{3+} ions*

Prominence of the $^5D_0 \rightarrow {}^7F_2$ transition intensity over that of $^5D_0 \rightarrow {}^7F_1$ indicates a distinctive feature: the preferential localization of Eu^{3+} within a distorted or irregular cation atmosphere, notably occupying Ca sites. This asymmetry amplifies the intensity of the $^5D_0 \rightarrow {}^7F_2$ transition, which is advantageous for achieving high-quality red light emission. Conversely, the relatively weaker intensities of transitions from ^5D_J (J = 1, 3, 4) contribute to the desirability of obtaining optimal red emission characteristics.

In the pursuit of enhanced red emission, the doping concentration of metal ions emerges as a critical determinant in the properties of luminescent materials. Thus, a comprehensive investigation into the optimal Eu^{3+} ion doping concentration within $CaMoO_4$ phosphors were conducted. This exploration involved the comparison of photoluminescence (PL) intensities obtained at one excitation wavelengths of 392 nm and the second excitation wavelength of 462 nm. Figure 4 illustrates the comparative PL intensity analysis of $CaMoO_4:xEu^{3+}$ phosphors (prepared by SSM), providing insights into the optimal Eu^{3+} ions concentration for amplified red emission characteristics.

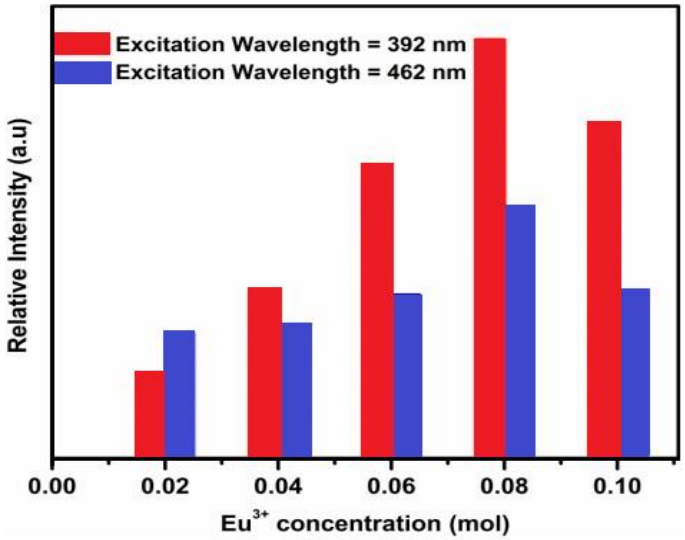

Figure 4. *Emission intensities of Eu^{3+} doped $CaMoO_4$ phosphors at 392 nm and 462 nm excitation respectively, analysed by varying Eu^{3+} concentrations.*

At 392 nm (near-UV) and 462 nm (blue), the brightness of the phosphors increases with more Eu^{3+} added until it hits a peak at 0.08 content. After that, adding more Eu^{3+} actually makes the brightness decrease. Interestingly, when we compare the brightness of the phosphors at these two wavelengths, we find that the ones excited at 392 nm (near-UV) are generally brighter than those excited at 462 nm (blue), regardless of the Eu^{3+} concentration.

Even though the brightest red light is seen at 0.08 mol% Eu^{3+} for both wavelengths, it's important to note that the brightness at 392 nm is much higher than at 462 nm. This implies that these phosphors may be particularly advantageous for producing red light in near UV-based white LEDs, rather than in blue GaN-based white LEDs. So, the best amount of Eu^{3+} to be doped in $CaMoO_4$ to get really bright red light is 0.08 mol%.

Reduction in the intensity of photoluminescence (PL) that is seen at concentrations higher than 0.08 mol%, this could be attributed to the energy exchange interaction between many excited Eu^{3+} ions. This quenching mechanism in europium-activated phosphors is generally ascribed to energy movement amongst the rare earth activators used like Eu^{3+} ions, this leads energy of excitation towards adjacent quenching sites (traps), which are frequently identified as defects or impurities within the lattice structure. Additionally, concentration quenching could be influenced by the method of synthesis. The microwave aided solid-state metathesis synthesis (SSM) process at room temperature likely facilitated an uniform environment for Eu^{3+} activators, enhancing their distribution within the host material. This, in turn, reduces the likelihood of energy transfer between neighboring Eu^{3+} ions, leading to quenching.

FTIR analysis

The figure 5 shows the Fourier Transform Infrared Spectroscopy spectra of $CaMoO_4:xEu^{3+}$ (for different concentration of x in mol).

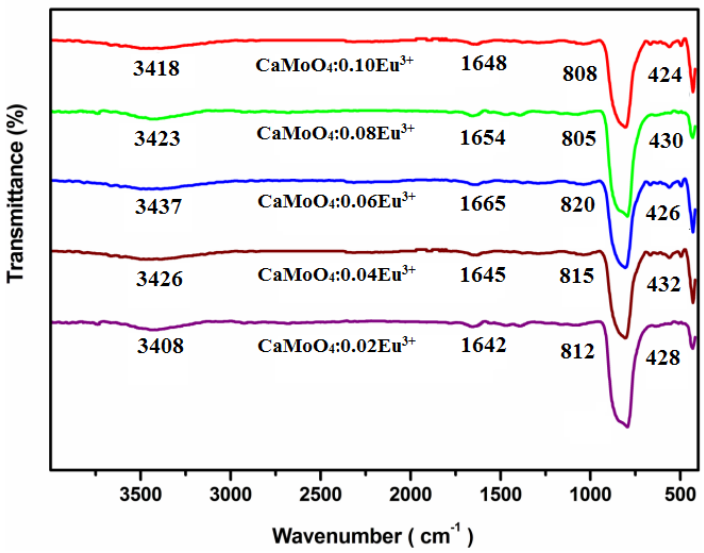

Figure 5. *FTIR spectra of $CaMoO_4:xEu^{3+}$*

From the graph it is easily observed that there is feeble absorption band is found nearby 428 cm^{-1}, bending vibration of Mo-O bonds is the cause behind this. Beside this the figure shows that very broad strong absorption band is about 812 cm^{-1} and this is because of the antisymmetric stretching vibrations of O-Mo-O. The stretching vibration of O-H bonds is responsible for the feeble absorption band at 3423 cm^{-1}, but the bending vibrations of H-O-H in water that is absorbed from the air are responsible for the bands about 1600 cm^{-1}.

Given the comparability of photoluminescence excitation (PLE) spectra with absorption spectra, it is reasonable to attribute the excitation band and peak in the PLE spectra to a singular absorption process. To further explore the energy absorption, one more characteristics of $CaMoO_4:xEu^{3+}$ is studied which is illustrated in Figure 6 that is Diffuse Reflectance Spectra (DRS). The DSR is measured for three different concentration of Eu^{3+} that is for x = 0.02, 0.08 and 0.10 mol % phosphors. The wavelength range from 220 nm to 350 nm displays the absorption band in the spectra, corresponding to the combined ligand to metal (combination of O-Mo) charge transfer (CT) in the MoO_4^{2-} group and transfer of electron from oxygen (O^{2-}) to europium (Eu^{3+}). are attributed to the 4f-4f electron transitions of Eu^{3+} ions is due to the two absorptions at wavelength 394 nm and 464 nm . The maximum absorption observed for $CaMoO_4:xEu^{3+}$ is steady with the results obtained in the excitation spectra.

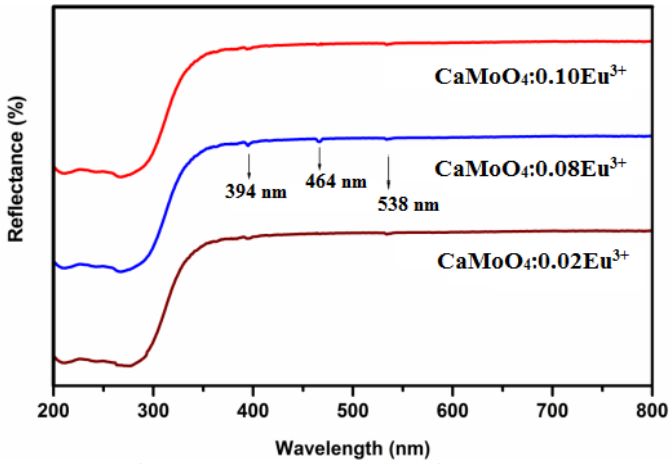

Figure 6. *DRS of $CaMoO_4:xEu^{3+}$ Phosphors for the Eu^{3+} concentration as 0.02, 0.08 and 0.10 mol%.*

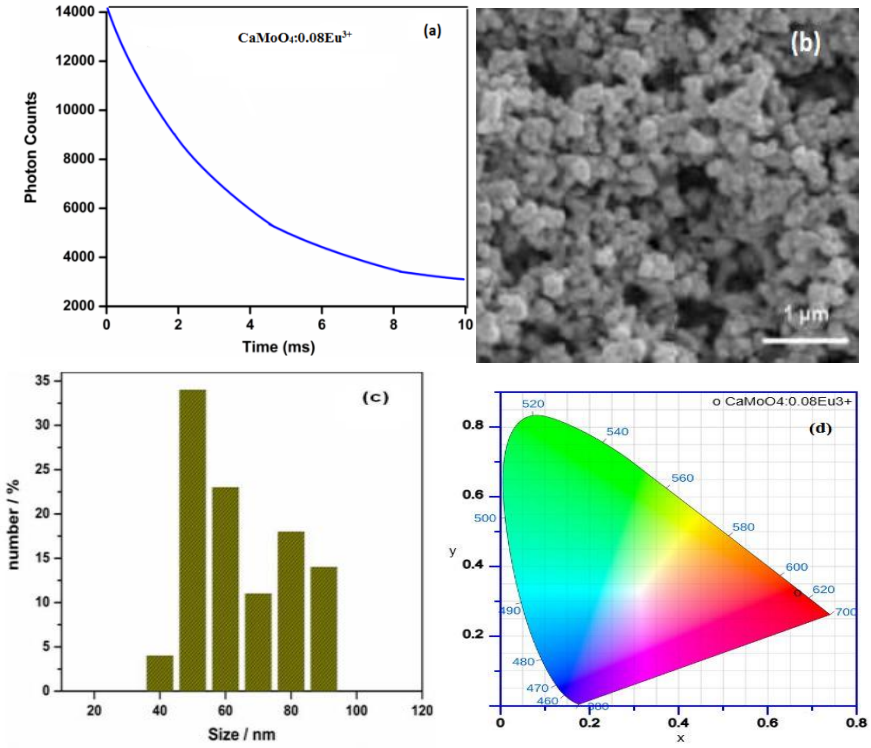

Figure 7. *(a) decay curve of $5D_0 \rightarrow 7F_2$ transitions at 618 nm of Eu^{3+} ions of $CaMoO_4:xEu^{3+}$ phosphor. (b) SEM image of CaMoO4:xEu^{3+} (c) Particle size distribution of $CaMoO_4:xEu^{3+}$ (d) CIE chromaticity diagram for $CaMoO_4:0.08Eu^{3+}$ phosphor (λex=392 nm).*

Successfully prepared via microwave assisted SSM route at room temperature are well-crystalline Eu^{3+} activated CaMoO4 phosphor powders with a scheelite-type structure. The FTIR spectra exhibit wide absorption band corresponding to the vibrational energy of MoO_4^{2-}. Under 392 nm excitation wavelength, the $CaMoO_4:xEu^{3+}$ phosphor demonstrates robust red emission at wavelength around 618 nm, attributed to forced electric dipole transitions. 0.08 mol % is the optimal concentration of Eu^{3+} that can be doped in $CaMoO_4$ to get immense emission of red color. Notably, intensity of emission spectra of $CaMoO_4:xEu^{3+}$ when excited at 392 nm surpasses that when excited at 462 nm, suggesting its suitability for one component that emits light having wavelength corresponding to red color in wLEDs over blue GaN-based counterparts. These characteristics position $CaMoO_4:xEu^{3+}$ that is synthesised by SSM using microwave as a promising material white LEDs. The fluorescence lifetime analysis (depicted in Figure 7 (a)) of the $^5D_0$ excited state of Eu^{3+} in $CaMoO_4:xEu^{3+}$ reveals a decay curve for $^5D_0 \rightarrow {}^7F_2$ (618 nm) fitting snugly to a single exponential function, with a determined lifetime of 0.401 ms. Additionally, the surface morphology (Figure 7 (b)) underscores the uniformity and suitability of the atoms, exhibiting a fine size distribution with an average radius of 25.5 nm as shown in Figure 7 (c), thus indicating their compatibility in developing solid-state based lighting devices.

5. CIE diagram

The CIE diagram (figure 7(d)) effectively showcases the red emissions exhibited by the phosphor particles upon excitation at a single wavelength (λ_{ex}=392 nm), affirming the potential of the $CaMoO_4:0.08Eu^{3+}$ sample as a favorable component white LEDs. The CIE chromaticity coordinates is x = 0.678 and y = 0.322 for $CaMoO_4:0.08Eu^{3+}$ phosphor, this data matches with the standard chromaticity coordinate values of NTSC. The standard chromaticity coordinate values as per NTSC is x = 0.668 and y = 0.323.

6. Conclusion

In summary, we have developed the $CaMoO_4$ phosphors by means of a simple solid state metathesis synthesis method that processed in a domestic microwave oven .Eu^{3+} was used as dopant in the present sample. The XRD, FT-IR spectroscopy, UV–vis absorption spectroscopy, DSR and PL measurements, while FE-SEM was used to investigate the morphology of the crystals of the presented phosphor prepared by using microwave assisted SSM synthesis method. The effects of change in concentration of dopant, including the change in excitation wavelength of $CaMoO_4$ were investigated systematically. Successfully prepared via microwave assisted SSM route are well-crystalline Eu^{3+} activated $CaMoO_4$ phosphor powders with a scheelite-type structure (obtained by FE-SEM). $CaMoO_4$:xEu^{3+} phosphors when excited by wavelength 392 nm, results the prominent absorptions at two wavelength 392 nm and 462 nm. The study highlights the consistent spectroscopic properties of $CaMoO_4$ phosphors under near-UV excitation, emphasizing the transition of Eu^{3+} from $^5D_0 \rightarrow {}^7F_2$ at wavelength 618 nm. Variations in emission intensity across different doping levels underscore the sensitivity of this transition to local environmental factors, particularly the symmetry around the Eu^{3+} ions. The CIE diagram effectively showcases the red emissions exhibited by the phosphor particles upon excitation at a single wavelength (λ_{ex} = 392 nm), affirming the potential of the $CaMoO_4$:xEu^{3+} phosphor as a promising component for near-UV InGaN-based white LEDs.

Financing and Declaration of Conflict of Interests:

The authors don't have any conflict of interest among them. The authors certify that they have NO affiliations with or involvement in any organization or entity with any financial interest or non-financial interest (such as personal or professional relationships, affiliations, knowledge, or beliefs) in the subject matter or materials discussed in this manuscript.

Ethical Approval:

This article does not contain any studies with human participants or animals performed by any of the authors.

References

1. H. A. Höppe, "Recent developments in the field of inorganic phosphors," Angewandte Chemie—International Edition, vol. 48, no. 20, pp. 3572–3582, 2009.
2. R.-J. Xie, N. Hirosaki, K. Sakuma, Y. Yamamoto, and M. Mitomo, "Eu2+-doped Ca-α-SiAlON: a yellow phosphor for white light-emitting diodes," Applied Physics Letters, vol. 84, no. 26, pp. 5404–5406, 2004.
3. Q. Dai, M. E. Foley, C. J. Breshike, A. Lita, and G. F. Strouse, "Ligand-passivated Eu:Y2O3 nanocrystals as a phosphor for white light emitting diodes," Journal of the American Chemical Society, vol. 133, no. 39, pp. 15475–15486, 2011.
4. B. Shao, J. Huo, H. You, Prevailing strategies to tune emission color of lanthanide-activated phosphors for WLED applications, Adv. Opt. Mater., 7 (2019) 1900319.
5. G.B. Nair, H.C. Swart, S.J. Dhoble, A review on the advancements in phosphor-converted light emitting diodes (pc-LEDs): Phosphor synthesis, device fabrication and characterization, Prog. Mater Sci., 109 (2020) 100622.
6. X. Ren, X. Zhang, N. Liu, L. Wen, L. Ding, Z. Ma, J. Su, L. Li, J. Han, Y. Gao, 22 White light-emitting diode from Sb-doped p-ZnO nanowire arrays/n-GaN film, Adv. Funct. Mater., 25 (2015) 2182-2188.
7. J.-H. Gwak, S. H. Park, J. E. Jang et al., "Synthesis and modification of red oxide phosphors for low voltage excitation," Journal of Vacuum Science & Technology B:, vol. 18, article 1101, 2000.

8. G. Wakefied, E. Holland, P. J. Dobson, and J. L. Hutchison, “Luminescence properties of nanocrystalline Y2O3:Eu,” Advanced Materials, vol. 13, no. 20, pp. 1557–1560, 2001.
9. Q. Tang, Z. P. Liu, S. Y. Li, S. Y. Zhang, X. M. Liu, and Y. T. Qian, “Synthesis of yttrium hydroxide and oxide nanotubes,” Journal of Crystal Growth, vol. 259, no. 1-2, pp. 208–214, 2003.
10. V. Dubey, J. Kaur, S. Agrawal, N. S. Suryanarayana, and K. V. R. Murthy, “Synthesis and characterization of Eu3+ doped SrY2O4 phosphor,” Optik, vol. 124, no. 22, pp. 5585–5587, 2013.
11. S.-J. Park, C.-H. Park, B.-Y. Yu, H.-S. Bae, C.-H. Kim, and C.-H. Pyun, “Structure and luminescence of SrY2O4:Eu,” Journal of the Electrochemical Society, vol. 146, no. 10, pp. 3903–3906, 1999.
12. J. Zhang, Y. Wang, L. Guo, and Y. Huang, “Vacuum ultraviolet-ultraviolet, X-ray, and near-infrared excited luminescence properties of SrR2O4:RE3+ (R = Y and Gd; RE = Tb, Eu, Yb, Tm, Er, and Ho),” Journal of the American Ceramic Society, vol. 95, no. 1, pp. 243–249, 2012.
13. J. L. Ferrari, A. M. Pires, and M. R. Davolos, “The effect of Eu3+ concentration on the Y2O3 host lattice obtained from citrate precursors,” Materials Chemistry and Physics, vol. 113, no. 2-3, pp. 587–590, 2009.
14. Q. Xiao, Y. Liu, Y. Zhong, and W. Zhu, “A citrate sol-gel method to synthesize Li2ZrO3 nanocrystals with improved CO2 capture properties,” Journal of Materials Chemistry, vol. 21, pp. 3838–3842, 2011.
15. S. Ray, P. Pramanik, A. Singha, and A. Roy, “Optical properties of nanocrystalline Y2O3:Eu3+,” Journal of Applied Physics, vol. 97, no. 9, Article ID 094312, 2005.
16. J. Wan, Z. Wang, X. Chen, L. Mu, and Y. Qu, “Shape-tailored photoluminescent intensity of red phosphor Y2O3:Eu3+,” Journal of Crystal Growth, vol. 284, no. 3-4, pp. 538–543, 2005.
17. M. R. Davolos, S. Feliciano, A. M. Pirez, R. F. C. Marquez, and M. Jafelicci Jr., “Solvothermal method to obtain europium-doped yttrium oxide,” Journal of Solid State Chemistry, vol. 171, no. 1-2, pp. 268–272, 2003.
18. K. Y. Jung, C. H. Lee, and Y. C. Kang, “Effect of surface area and crystallite size on luminescent intensity of Y2O3:Eu phosphor prepared by spray pyrolysis,” Materials Letters, vol. 59, no. 19-20, pp. 2451–2456, 2005.
19. J. T. Ingle, R. P. Sonekar, S. K. Omanwar, Y. Wang, and L. Zhao, “Combustion synthesis and VUV photoluminescence studies of borate host phosphors YBO3:RE3+ (RE = Eu3+, Tb3+) for PDPs applications,” Combustion Science and Technology, vol. 186, no. 1, pp. 83–89, 2014.
20. K. Xu, G. He, G. Liu, Z. Han, and J. Lia, “Combustion synthesis of Eu2+ doped β-SiAlON phosphors by salt assistance,” ECS Journal of Solid State Science and Technology, vol. 2, no. 11, pp. R230–R232, 2013.
21. José Miranda de Carvalho et. al, “Microwave-Assisted Preparation of Luminescent Inorganic Materials: A Fast Route to Light Conversion and Storage Phosphors” 2021 May 13. doi: 10.3390/molecules26102882
22. P. Biswas, V. Kumar, V. Sharma, A.K. Bedyal, N. Padha, H.C. Swart, “Potential of Sm3+ doped LiSrVO4 nanophosphor to fill amber gap in LEDs” Phys. B 535, 221 (2018)